JOURNAL OF MATERIALS SCIENCE 13 (1978) 1411–1418

Effect of bond angle on mixed-mode adhesive fracture

W. D. BASCOM, J. OROSHNIK
Polymeric Materials Branch, Naval Research Laboratory, Washington, D.C. 20375, USA

A maximum in mixed-mode adhesive fracture energy has been observed at bond angles of 45° using scarf-joint test specimens. It is shown here that by reducing the adherend surface roughness from 1.2 μm CLA roughness (milled surfaces) to 0.08 μm CLA roughness (polished surfaces) the fracture energy becomes a linear function of bond angle (no maximum at 45°) and there is an overall decrease in fracture energy at all bond angles. These results are discussed in terms of crack initiation being "focused" into the interfacial region and a pinning of crack-tip shear displacements by the surface roughness of the milled adherends which does not occur for the polished adherends.

1. Introduction

Studies of the adhesive fracture of polymer/metal bonds under combined tensile and shear (mixed-mode) loading have been reported by Trantina [1, 2], Bascom *et al.* [3], Bascom and Timmons [4], and Mulville *et al.* [5, 6]. Trantina reported mixed-mode strain energy release rates $\mathcal{G}_{(I,II)_c}$ for aluminium/epoxy-polyamide polymer bonds using the "scarf-joint" specimen illustrated in Fig. 1 for which he had developed a finite element stress analysis. Bascom *et al.* used this specimen and Trantina's analysis to determine adhesive $\mathcal{G}_{(I,II)_c}$ values for aluminium bonded with an anhydride-cured epoxy [3] and a variety of elastomer-modified epoxy and commercial structural adhesives [4]. They confirmed the observation made by Trantina that failure always occurred near the adhesive/adherend boundary and were able to demonstrate that the locus of failure was in the adhesive polymer a few hundred Ångstroms from the interface. They also found a distinct but complex dependence of $\mathcal{G}_{(I,II)_c}$ on the adherend surface roughness. Mulville *et al.* [5, 6] studied crack propagation along the boundary between plates of epoxy polymer cast onto plates of aluminium. They observed that under mixed-mode loading, failure occurred near the boundary but in the epoxy, and that $\mathcal{G}_{(I,II)_c}$ increased systematically with the roughness of the aluminium.

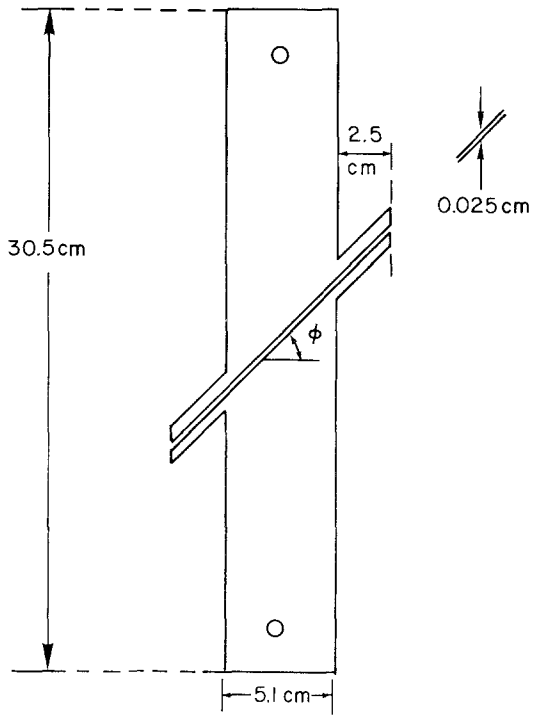

Figure 1 "Scarf-joint" specimen for mixed-mode adhesive fracture testing. The tabs at the bond line are used to clamp the specimen while the adhesive is curing.

Bascom *et al.* [4] have reported data on the effect of bond angle (ϕ in Fig. 1) on $\mathcal{G}_{(I,II)_c}$ which indicated a maximum in adhesive fracture

toughness at $\phi = 45°$. This effect is examined in detail in the work reported here and shown to result from adherend surface roughness inhibiting interfacial crack propagation.

2. Experimental

The principal adhesive polymer used in this study was a tetra-functional epoxy based on *bis* (N, N-di (2, 3-epoxy propyl)-4-aminophenyl) methane (TGMBA) cured with 4,4′ diaminodiphenylsulfone (DDS) known commercially as NARMCO 5208 (Narmco Materials Inc., Costa Mesa, CA). The resin is applied as a melt and cured as follows; 93° C, 20 h; 121° C, 3 h; 149° C, 2 h; 177° C, 2 h; 204° C, 4 h. This heating schedule avoids exothermic heat build-up. The other adhesive polymers for which data is presented have been described elsewhere [3, 4] and include a piperidene-cured diglycidyl ether bisphenol A epoxy (DGEBA, DER 332, Dow Chemical Co.), a piperidene-cured DGEBA containing 15 wt% carboxy-terminated butadiene acrylonitrile (CTBN, B.F. Goodrich, Cleveland) and a commercial CTBN-modified epoxy structural adhesive (manufacture discontinued).

The scarf-joint specimens were cut from 1.3 cm aluminium alloy (5086) plate and had the dimensions given in Fig. 1. The bonding surfaces were given a fine mill finish (centre-line-average, CLA, 1.2 μm roughness) or were polished to a mirror finish (0.08 μm CLA roughness). The specimens with the milled finish were cleaned by an acid-chromate etch [7], water-rinsed and air-dried. The polished specimens were cleaned by light abrasion with a 0.1 μm alumina–water slurry on a metallographic polishing wheel, followed by rinsing in a strong tap water stream to remove alumina particles, plus a final rinse with distilled water.

In previous studies with the scarf-joint specimen it had been possible to form a pre-crack by wedging open one of the side arms. However, in the tests with the TGMBA resin it was found that uncontrolled damage (microcracking) was occurring ahead of the pre-crack. Consequently, it was necessary to "build-in" a pre-crack by embedding a razor blade in the bond line. Double-edge, polytetrafluoroethylene (PTFE) coated blades ("Platinum Plus", Gillette) were used and were reported by the manufacturer to have an edge radius of 50 to 200 Å. The blades were broken in half and placed in the bond line at the specimen edge before the resin was applied. Details about the nature of the pre-crack produced by the razor blade inserts are given in the Section 3.

The TGMBA resin was applied by heating the aluminium specimens above the resin melting point and wiping the resin onto the bonding surface until more than sufficient resin had been accumulated to fill the bond to a thickness of 4 mil (0.01 cm).

3. Results

The adhesive $\mathcal{G}_{(I,II)_c}\phi$ values obtained for the tetra-functional epoxide polymer (TGMBA-DDS) using the scarf-joint specimen are plotted in Fig. 2 and include data taken at 22 and 150° C. In both cases there appears to be a maximum in fracture energy at $\phi = 45°$. Test data obtained using the scarf-joint specimen, both in this study and in earlier work, typically have a high standard deviation as is evident from Fig. 2. However, the average values of $\mathcal{G}_{(I,II)_c}\phi$ for separate runs of five specimens per angle differed by less than 20%. Evidently, the scarf-joint fracture energies are reproducible, but there is some uncontrolled factor causing wide specimen-to-specimen deviations.

The maximum in adhesive $\mathcal{G}_{(I,II)_c}\phi$ at $\phi = 45°$ had been reported previously for other polymers and these results are presented in Fig. 3 for purposes of comparison. The adhesives used were a piperidene-cured DGEBA epoxy polymer, with and without a CTBN modifier, and a commercial CTBN-modified DGEBA adhesive. Included in Fig. 3 are the results for these polymers for mode-I ($\phi = 0°$) and mode-II ($\phi = 90°$) adhesive fracture. The high $\mathcal{G}_{I_c}$ values of the CTBN-modified polymers are characteristic of these elastomer-toughened materials [4,8] but there is a considerable decrease in their toughness in mixed-mode loading and this anomaly is discussed elsewhere [9]. In mode-II loading all the polymers exhibited high adhesive toughness values and the test probably underestimates $\mathcal{G}_{II_c}$ as discussed below.

It was noticed in the scarf-joint tests of the TGMBA polymer that although failure occurred very close to one interface for all bond angles, the resin layer left on the adherend was much thinner for the 45° specimen than for the 30° or 60° specimens. This observation is illustrated by the photograph in Fig. 4 which shows the greater reflectivity of the 45° specimen surface.

Since failure was occurring closer to the metal boundary at 45° than at the other angles, and since

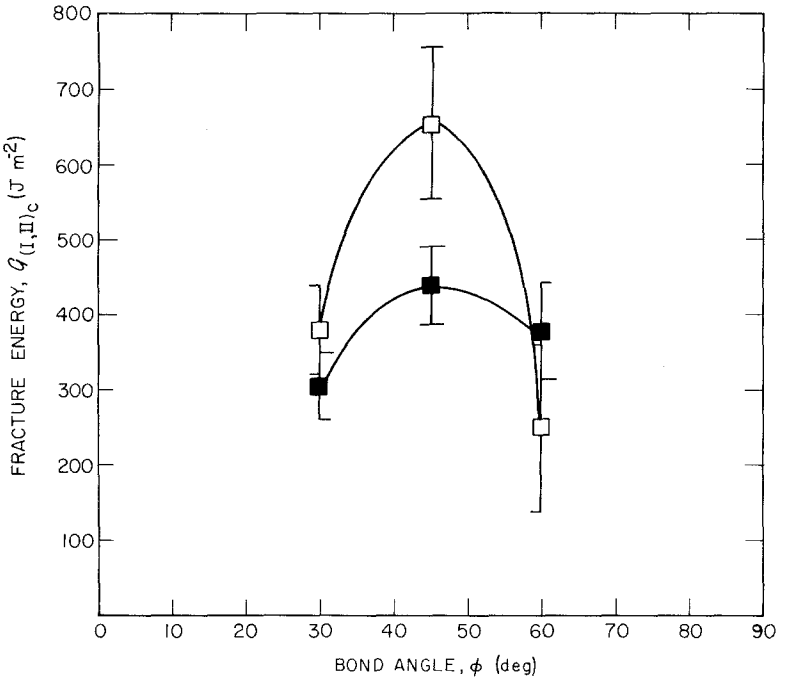

Figure 2 Effect of bond angle on the adhesive fracture energy of the TGMDA-DDS polymer for milled (and etched) adherends tested at 22° C (□) and 150° C (■).

surface roughness has a large effect on $\mathcal{G}_{(I,II)_c}\phi$ [3, 5] it was decided to study the effect of bond angle on adhesive toughness using polished adherends. Previous work [3] with scarf-joint specimens which had the bonded surface polished to 0.08 μm CLA roughness indicated that this level of roughness was too low to affect fracture.

The results for the TGMBA polymer using polished adherends are given in Fig. 5 and show that there is no longer a maximum in $\mathcal{G}_{(I,II)_c}$ at $\phi = 45°$. Furthermore, a least-squares fit of the data extrapolates to a $\mathcal{G}_{I_c}$ value ($\phi = 0°$) of 75 J m^{-2} which compares favourably with the value of 83 J m^{-2} obtained for this polymer using the tapered double cantilever beam specimen [10].

Post-failure examinations were made of frac-

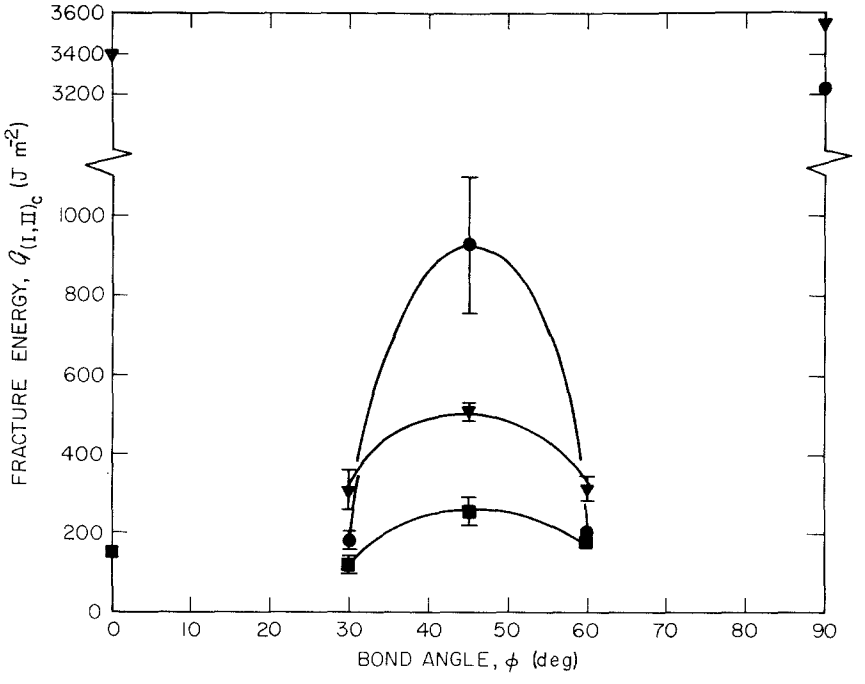

Figure 3 Effect of bond angle on the adhesive fracture energy of various epoxy polymers; ■, piperidene-cured DGEBA; ▼, piperidene-cured DGEBA with 15% CTBN; ●, a commercial DGEBA-CTBN film adhesive (adherends milled and etched).

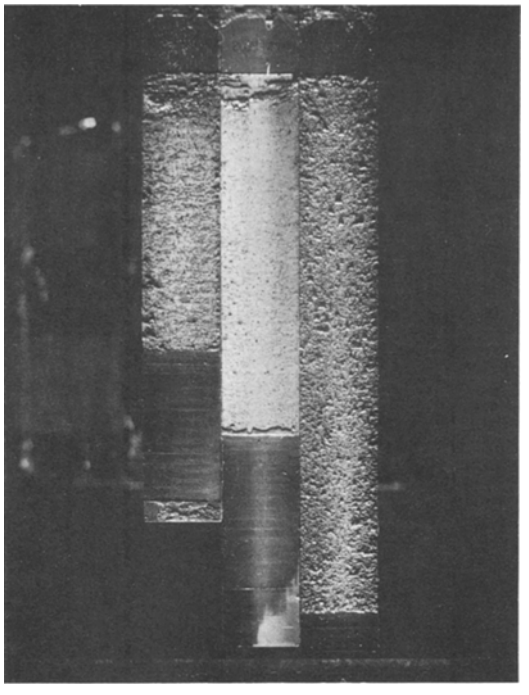

Figure 4 Comparison of the milled adherends after fracture showing a considerably thicker resin layer on the 30° (right) and 60° (left) specimens compared to the 45° specimen (centre).

ture specimens with emphasis on the region of crack initiation near the razor blade insert. The low magnification photographs of Fig. 6 show the two specimen halves (Fig. 6a) and a SEM view near the razor edge (Fig. 6b). The photograph in Fig. 7 identifies the principal features on the "adherend" side of the failure. The schematic drawing of Fig. 8 illustrates the region of crack initiation ("adhesive"

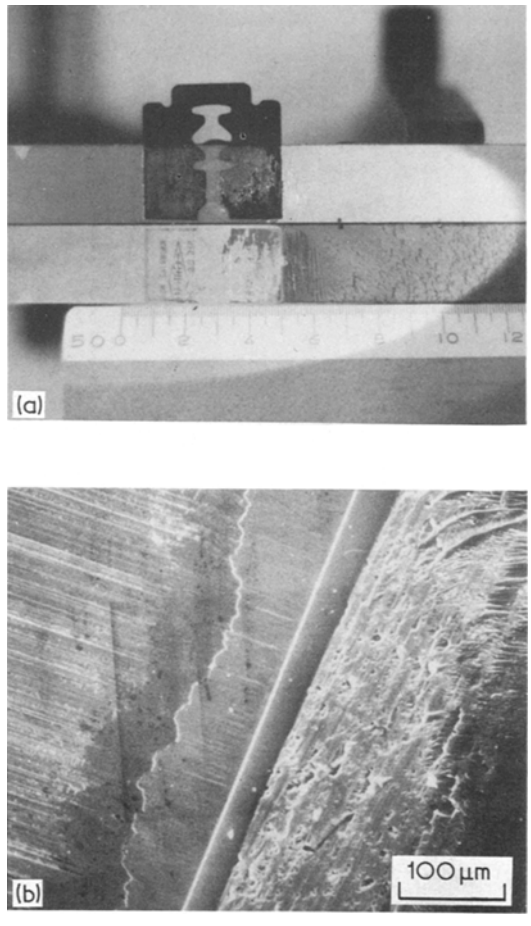

Figure 6 Post-failure photographs of razor initiated failure (a) View of razor insert. (b) SEM photograph of razor edge (left), mode-I fracture from razor (centre) and "interfacial" failure region (right). Milled and etched adherends.

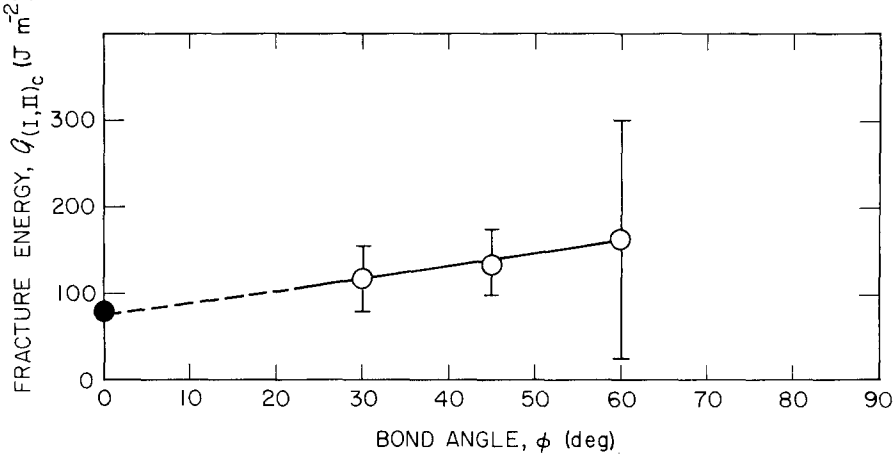

Figure 5 Effect of bond angle on the adhesive fracture energy of the TGMBA-DDS polymer for polished adherends.

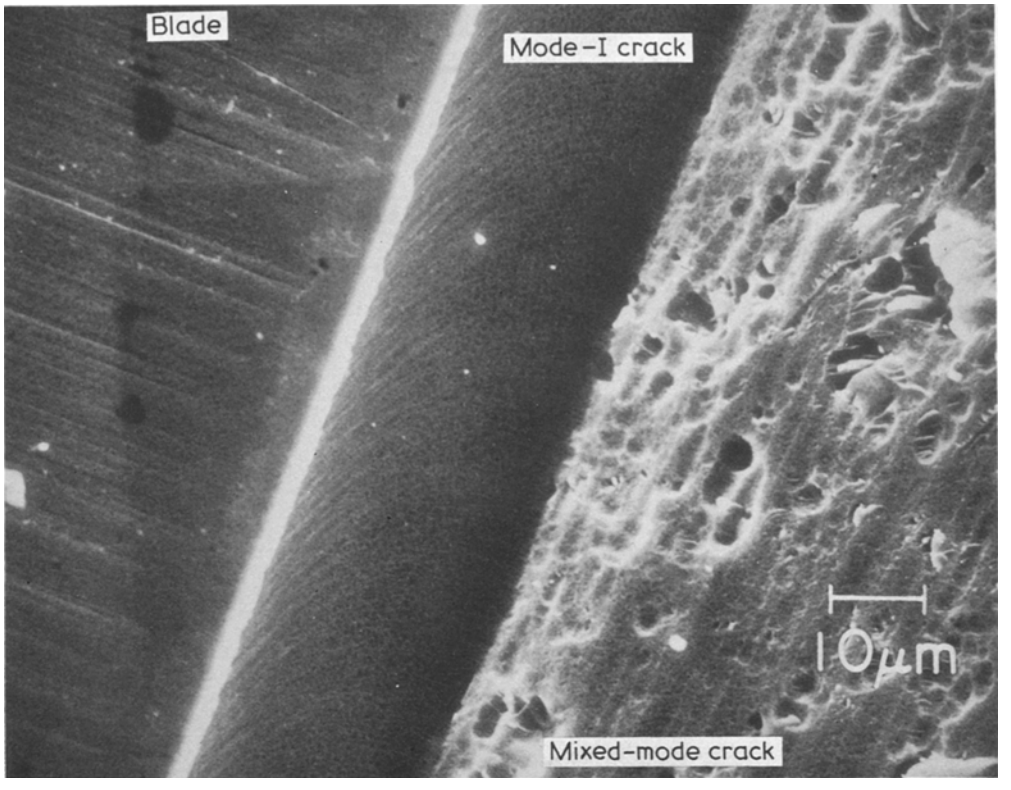

Figure 7 SEM photograph of the "adherend" region of crack initiation.

side) and indicates the imprint of the blade (ABCD), a mode-I crack from the blade edge to the adhesive/adherend boundary (DE) and the failure plane along the boundary (EF). In earlier work, Trantina [1] and Bascom *et al.* [3] had found that failure of the scarf-joint specimen with a centre-of-bond pre-crack involved mode-I cracking from the pre-crack tip to the adhesive/adherend boundary. Then, at a higher load, the entire specimen failed catastrophically near the interface. A similar sequence appears to have occurred with the razor blade insert.

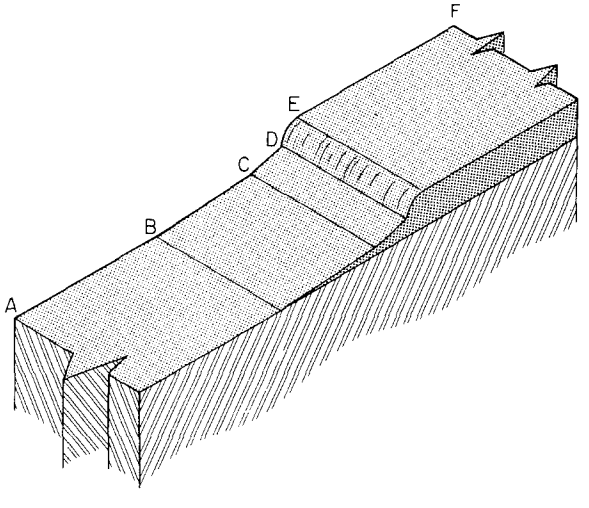

Figure 8 Schematic of "adhesive" side of fracture. Areas from A to D are imprint left by razor, region DE is mode-I crack from razor edge, and EF is region of "interfacial" failure.

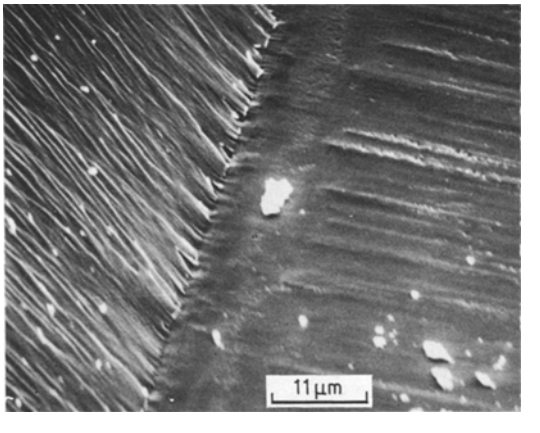

Figure 9 SEM photograph of mode-I failure on the "adhesive" side of the failure surface showing the imprint left by the razor (right) and the tear marks of the mode-I failure surface (left).

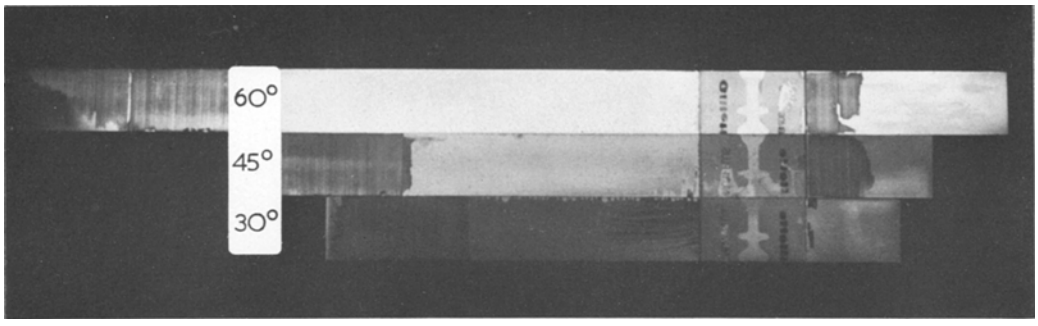

Figure 10 Comparison of polished adherends after fracture showing effect of residual adhesive layer on surface reflectivity.

The mode-I crack did not initiate from the blade edge but slightly behind it; by about 0.3 to 0.5 μm as estimated from SEM photographs. In Figs. 6b and 7 note the overhang of the blade edge which appears bright due to charging in the SEM electron beam. Fig. 9 shows the corresponding position on the "adhesive" side of the fracture and note the slight undercutting where the blade edge had pulled out of the resin. Note also the ribbed structure of the mode-I fracture surface (LHS of Fig. 9) and the very rough surface in the region of "interfacial" cracking (mixed-mode crack area of Fig. 7). There was a discernable layer of polymer on this region of interfacial cracking so that failure

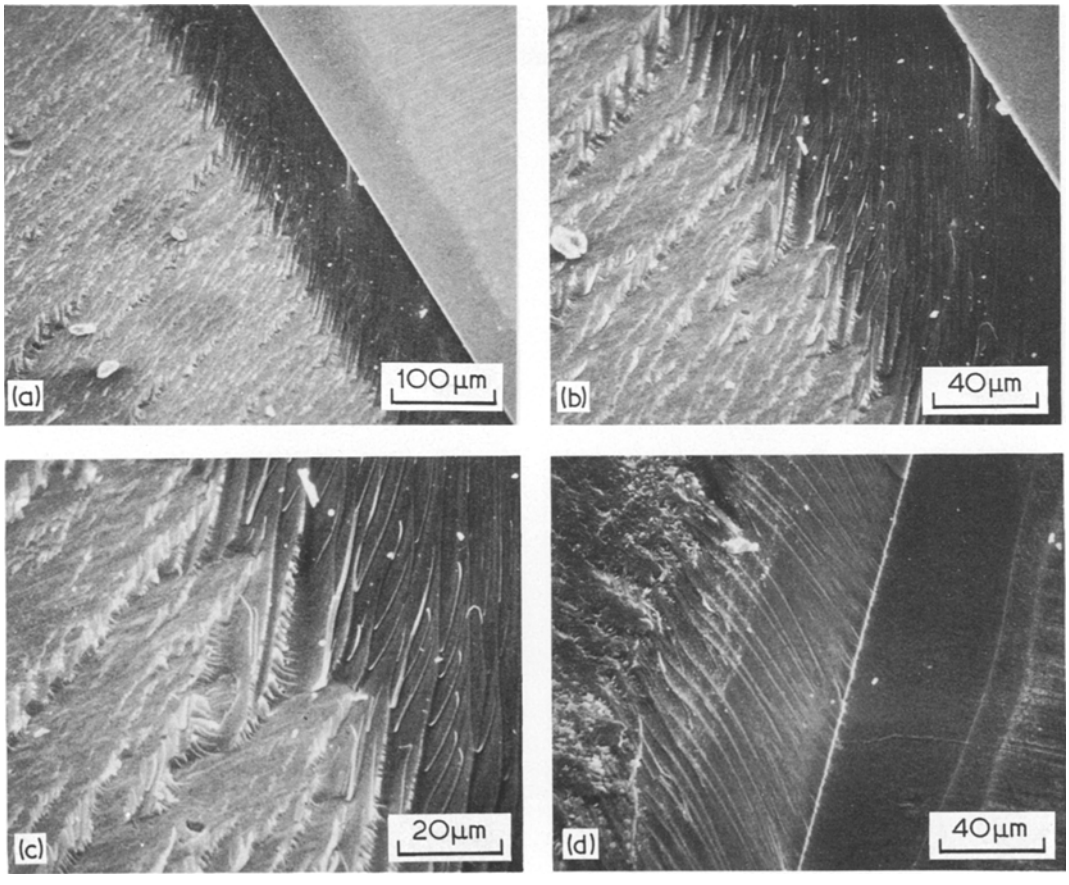

Figure 11 SEM post-failure photographs of polished adherend surfaces in the vicinity of the razor edge. (a to c) "adherend" surface, (d) "adhesive" surface.

had actually occurred in the adhesives but close enough to the metal to replicate the machine markings on the underlying aluminium.

The fractured surfaces of the polished adherend specimens were viewed in reflected light and interference coloration indicated a film of resin had been left on the "adherend" side of the failure at all bond angles. However, as illustrated in Fig. 10, the thickness of the residual resin layer was greatest for $\phi = 30°$ and least at $\phi = 60°$ as judged by the difference in reflectivities. Note that this result differs from that with the mill finish adherends for which the thinnest residual film occurred at $\phi = 45°$.

The SEM post-failure appearance of the polished adherend specimens in the vicinity of the razor edge is given by the photographs in Fig. 11. As had been observed for the milled specimens, the razor edge appears to overhang the mode-I failure surface. Also, the ribbed tearing of the mode-I failure surface is again evident. The mixed-mode, "interfacial", region is characterized by shear tearing that leaves strips of polymer on the adherend (Figs. 11a to c and channels in the adhesive failure surface (LHS, Fig. 11d).

4. Discussion

It is evident that the maximum in scarf-joint adhesive fracture toughness at the bond angle of 45° is associated with an effect of adherend roughness on the initiation of mixed-mode, "interfacial", crack propagation. Polishing the aluminium adherend surfaces eliminated the maximum at 45° and also lowered $\mathcal{G}_{(I,II)_c}$ at all three bond angles compared to the milled and etched specimens. Effects of surface roughness on mixed-mode adhesive toughness have been reported before [3, 5, 6]. They result first, because the locus of failure is "focused" into the interfacial region by the combined-stress loading, and secondly, because crack initiation is impeded by the adherend roughness. As pointed out by Mulville *et al.* [5, 6], the presence of a shear component drives the crack along the interface and the strain energy release rate for crack propagation along the interface increases systematically with surface roughness*.

There is a ready explanation for the maximum in $\mathcal{G}_{(I,II)_c}$ of the scarf-joint at $\phi = 45°$ if it can be assumed that the proximity of crack initiation

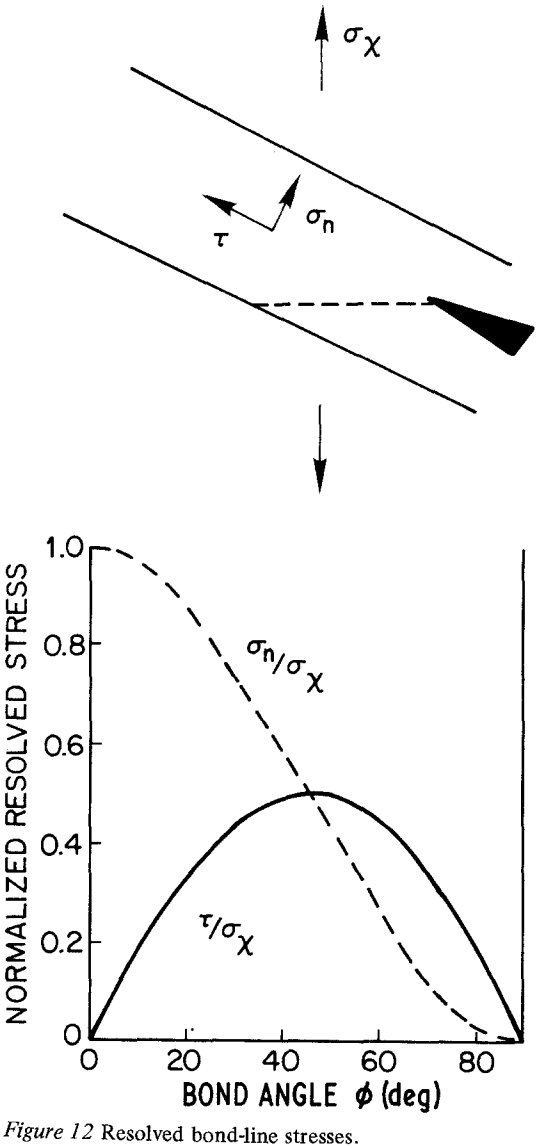

Figure 12 Resolved bond-line stresses.

to the adherend surface is determined by the magnitude of the shear component, τ, in the bond line. As illustrated in Fig. 12, the applied stress, σ_x, can be resolved into bond line stresses, one normal to the interface, σ_n, and one parallel to the interface, τ. These stresses are related to the bond angle by:

$$\sigma_n = \sigma_x \cos^2 \phi \quad (1)$$

$$\tau = \sigma_x \sin \phi \cos \phi \quad (2)$$

The normalized bond line stresses are plotted in Fig. 12.

Using Equations 1 and 2 it is possible to resolve

*Although increasing $\mathcal{G}_{(I,II)_c}$ with surface roughness is generally observed when comparing large changes in roughness, this trend may be reversed when comparing surfaces of similar CLA roughness but which differ in the sharpness or amplitude of the asperites [3].

TABLE I

Adherends	ϕ	σ_x* (MPa)	τ (MPa)	σ_n (MPa)
Milled and etched	30°	25.1	10.78	18.84
	45°	34.8	17.39	17.39
	60°	33.0	14.18	8.24
Polished	30°	13.04	5.60	9.78
	45°	18.55	9.27	9.27
	60°	25.9	11.12	6.46

*Average of 5 to 6 specimens.

the bond line stresses at failure from the actual failure loads, P_c ($\sigma_x = P_c/A$, where A is the specimen cross-sectional area normal to the load direction) and the results are given in Table I. Comparisons of these values are valid since the crack lengths (and thus the net section areas) were approximately the same for all specimens.

In Table I the resolved shear stress is largest at $\phi = 45°$ for the milled adherend tests which is consistent with the argument that the shear component determines the proximity of failure to the adhesive/adherend boundary (i.e. Fig. 4). On the other hand, τ does not go through a maximum in the case of the polished adherends but increases steadily with bond angle and, as shown in Fig. 10, failure occurred closer to the adherend surface the greater the bond angle.

Viewed at a microscopic level, the actual crack-tip stress distributions are by no means as simple as the above analysis might suggest. The fact that the fracture energies were much lower for the polished adherends than for the milled specimens suggests that the shear component contributes to crack propagation in the absence of roughness but is much less effective when the adherend is roughened. The SEM photographs of "interfacial" failure from the milled surfaces (Figs. 6 and 7) suggest the resin was pulled out (tensile failure) of the surface grooves and pockets created by milling and etching the surface. On the other hand, the ridges left on the polished surfaces (Fig. 11) suggest localized, co-operative shear and tensile failure of the resin.

Adhesive fracture in pure mode-II loading leads to very high $\mathcal{G}_c$ values. Indeed, it is problematical whether a true mode-II (in-plane shear) failure can be observed. Mulville *et al.* [5] found that some tensile (mode-I) component was required for boundary crack propagation in their mixed-mode studies. The high $\mathcal{G}_{II_c}$ values reported previously [4] and plotted in Fig. 3 were obtained by shear loading bonded beams. Although the loading condition was mode-II, failure occurred by the formation of multiple microcracks along the bond line at an angle of about 45° to the loading direction. Referring to Fig. 5, it would be unrealistic to extrapolate the data to $\phi = 90°$ ($\mathcal{G}_{II_c}$) and in fact, the curve probably turns sharply upward as the ratio of $\mathcal{G}_{II}/\mathcal{G}_I$ is increased.

5. Conclusions

The large effect of surface roughness on mixed-mode adhesive fracture is further evidence of the strong role roughness can play in determining bond strength. The results of this study suggest that an important part of the "roughness effect" is due to a "pinning" of crack-tip shear displacements by the rugosity. The relationship between adherend roughness and bond strength is complicated because the relative magnitude of the shear component determines how close to the interface failure occurs, i.e., how deep into the roughness crack propagation must initiate. However, the ratio of shear to tensile component forces depends on joint geometry, i.e., bond angle in the case of the scarf-joint.

Acknowledgements

The authors are especially indebted to Dr D. R. Mulville and Dr D. L. Hunston of the Naval Research Laboratory.

References

1. G. G. TRANTINA, *J. Comp. Mater.* **6** (1972) 371.
2. *Idem*, T and AM Report 352, University of Illinois, Urbana (1971).
3. W. D. BASCOM, C. O. TIMMONS and R. L. JONES, *J. Mater. Sci.* **10** (1975) 1037.
4. W. D. BASCOM, R. L. JONES and C. O. TIMMONS, "Adhesion Science and Technology", part B, edited by L-H. Lee, (Plenum Press, New York, 1975).
5. D. R. MULVILLE, P. W. MAST and R. N. VAISHNAV, *Eng. Fracture Mech.*, 8 (1976) 555.
6. D. R. MULVILLE and R. H. VAISHNAV, *J. Adhesion* 7 (1975) 215.
7. N. J. DeLOLLIS, "Adhesives for Metals", (Industrial Press Inc., New York, 1970) p. 29.
8. W. D. BASCOM, R. L. COTTINGTON, R. L. JONES and P. PEYSER, *J. Appl. Polymer Sci.*, **19**, (1975) 2545.
9. W. D. BASCOM, D. L. HUNSTON, and C. O. TIMMONS, in preparation.
10. W. D. BASCOM and R. L. COTTINGTON, unpublished results (1976).

Received 27 June and accepted 7 October 1977.